Static Thermochemical Model of COREX Melter Gasifier

C. SRISHILAN and AJAY KUMAR SHUKLA

COREX is one of the commercial smelting reduction processes. It uses the finer size ore and semi-soft coal instead of metallurgical coke to produce hot metal from iron ore. The use of top gas with high calorific value as a by-product export gas makes the process economical and green. The predictive thermochemical model of the COREX process presented here enables rapid computation of process parameters such as (1) required amount of ore, coal, and flux; (2) amount of slag and gas generated; and (3) gas compositions (based on the raw material and desired hot metal quality). The model helps in predicting the variations in process parameters with respect to the (1) degree of metallization and (2) post-combustion ratio for given raw material conditions. In general reduction in coal, flux, and oxygen, the requirement is concomitant with an increase in the degree of metallization and post-combustion ratio. The model reported here has been benchmarked using industrial data obtained from the JSW Steel Plant, India.

https://doi.org/10.1007/s11663-017-1147-x

I. INTRODUCTION

THE process of reducing iron ores to iron is classified into two types: (1) direct reduction and (2) smelting reduction. The method chosen depends on the end product desired, namely, sponge iron or hot metal, respectively. The most widely used process to reduce iron ores to hot metal is the blast furnace route. The blast furnace route requires sintering as a preprocessing step and high-grade metallurgical coke for the reduction. The high cost and reduced availability of coking coal has resulted in research leading to development of new ways for reducing iron ore using noncoking coal. MIDREX, HYL, SL/RN, *etc*. are processes to produce direct reduced iron. On the other hand, COREX, HISMELT, *etc*. are processes to produce hot metal from iron ores without using coke as reported by Hasanbeigi *et al*.[1] Among them, COREX is one of the commercially viable processes. The generation of export gas and utilization of process gas through CO_2 stripping makes it more efficient, environmentally friendly (with reduction in CO_2 emission upto ~ 20 pct), and economic.[2]

The process initially known as the Kohl-Reduktion (KR) method was optimized further during 1970s by the German Korf Company and Voest Alpine International (VAI) resulting in the development of the COREX process. Industrial scale COREX 1000, 2000, and 3000 plants were installed at South Africa's ISCOR, South Korea's POSCO, and Pugang's Baoshan iron and steel group, in 1970, 1989, and 2007, respectively.[3]

The process flow of the COREX[4] is shown in Figure 1. It is a two-stage smelting reduction process. It consists of (1) a reduction shaft for reducing the lump ore and pellets and (2) a melter gasifier for final reduction of prereduced ores and gasification and devolatilization of coal. The gas generated from the melter gasifier is used for the reduction process in the reduction shaft. The shaft furnace is a counter current reactor, where lump ore and pellets are reduced to ~ 85 pct metallization; the material is then discharged at ~ 800 °C from the reduction shaft into the horizontal screw conveyors. It flows into the charging pipes of the melter gasifier. The reducing gas from the melter gasifier enters the shaft furnace at ~ 800 °C and exits the furnace top at ~ 450 °C. The melter gasifier, which completes the reduction and melting of prereduced ore, consists of a fluidized bed chamber resting on a liquid slag and a hot metal bath. Coarse coal along with coke is charged from the top of the melter gasifier and charred in a fluidized bed. Oxygen is injected *via* tuyeres around the circumference of the melter gasifier to form the raceway. In the raceway, oxygen reacts with charred coal to form CO. CO_2 is stripped from the top gas and recirculated to the shaft furnace along with the reducing

C. SRISHILAN and AJAY KUMAR SHUKLA are with the Department of Metallurgical and Materials Engineering, IIT Madras, Chennai 600036, India. Contact e-mail: c.srishilan@yahoo.com

Manuscript submitted June 23, 2017.
Article published online December 4, 2017.

gas for better utilization of the process gas. The export gas (~ 45 pct CO, 33 pct CO_2, 13.5 pct H_2, 1.5 pct CH_4) is also co-generated because of its high calorific value.[2]

Ever since COREX's advent, many academically and industrially relevant problems have been explored. Briefly, several researchers have modeled the process to predict the influence of input material on process parameters. The models developed so far are based on (1) static elemental heat and material balance equations operational in the melter gasifier of COREX process,[5] and (2) steady-state transport phenomena approaches to study the operational parameters.[6–9] The unsteady state model of the process developed by Pal *et al.*[10] has been used to study the transient behavior of the melter gasifier. The transport phenomena model for reduction shaft, developed by Wu and co-workers, is found to be useful too.[11–13] A shaft furnace has been examined using discrete element method (DEM) simulation.[14–20] Furthermore, turbulence models[21] have been employed to study gas and particle velocities, their distribution, and heat transfer pathways. The raceway of the melter gasifier has been studied using computational fluid dynamics (CFD) models[22–24] and heat balance approaches.[25] The burden distribution of the melter gasifier has been studied by CFD-DEM approach by Li *et al.*[26] Thermodynamic models of the process have been developed to predict hot metal and gas composition[27–29] and exergy losses.[30] Likewise, individual zones of the melter gasifier, namely, the free board zone,[31] moving bed,[32,33] hearth,[34] and cohesive zone,[35] are all of current interest and are being primarily studied using numerical models.

Nevertheless, a comprehensive model of the COREX process based on macroscopic heat and mass balance of input and output materials is still a challenge for researchers. Various static models[36–38] have been reported to study the effect of the post-combustion ratio and degree of metallization on the fuel and slag rates.

In the present work, a thermochemical model has been developed to calculate and predict the output parameters based on the input raw material data. The present model performs the material and heat balance and thermochemical calculations to predict the output hot metal, slag quantity, required coal consumption rate, gas volumes, and compositions. This model operates by splitting the top gas into two components: export gas and surplus gas; this is fed back along with the reducing gas to the reduction shaft. The influence of the variables like the degree of metallization and post-combustion ratio has been studied in a comprehensive manner. This model has been validated with the industrial data from the JSW Steel Plant, India.

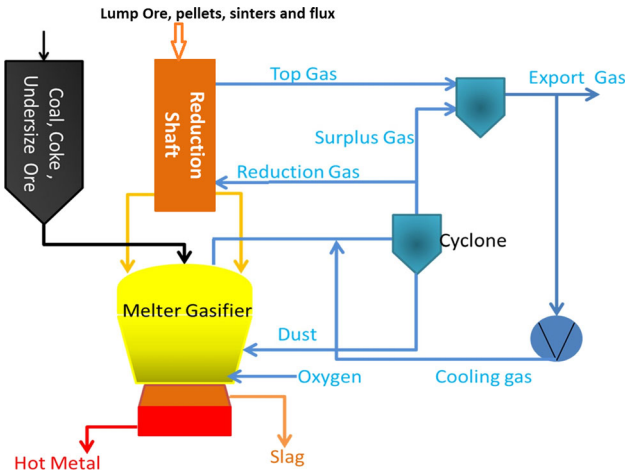

Fig. 1—Schematic representation of COREX process.

II. MODEL DESCRIPTION

The present thermochemical model performs material and heat balance of the elements entering and leaving the COREX process. The present model assumes the process to be operating at the steady state. A stoichiometric amount of oxygen is used to complete the coal combustion process in the melter gasifier. The melter gasifier gases are assumed to be in dynamic equilibrium with hot metal due to the very high temperature and rapid rate of reactions. The gas temperature and compositions are considered to be uniform. Post-combustion is incomplete due to the high-temperature dissociation reactions of CO_2 and H_2O.

The model considers the gas leaving the melter gasifier to be sent into the reduction shaft for pre-reduction of iron ore to wustite. The gas coming out of the reduction shaft is divided into two parts, namely, the (1) reducing gas and (2) surplus gas. The surplus gas is reverted back into the melter gasifier through the cyclones for stripping of CO_2 present in it. CO_2 reacts with the coal and produces CO, as shown in Figure 1. The reducing gas is then circulated to the reduction shaft for pre-reduction of ores.

A. *Material Balance*

Hot metal and slag consist of elements and oxides, respectively. Elemental balance for C, Fe, Si, Mn, S, P, H, N, O, Ca, and Mg and oxide balance for Al_2O_3 have been carried out. All the calculations are done on the basis of 1-kg mole of product Fe in the hot metal.

The elements with their sources and exit forms are shown in Table I. Balancing each element gives the stoichiometric information regarding slag, top gas, and surplus gas composition. An Fe balance calculation provides the mass of iron ore required (Eq. [1]). Carbon balance provides the active carbon needed for coal combustion, calculated using Eq. [2]:

$$M_{\text{ore}} = \frac{100 \times 160}{p^{\text{ore}}_{\text{Fe}_2\text{O}_3} \times 2} \qquad [1]$$

$$n^{\text{A}}_{\text{C}} = n^{\text{coal}}_{\text{C}} + n^{\text{L}}_{\text{CaCO}_3} + n^{\text{L}}_{\text{CaCO}_3} + n^{\text{D}}_{\text{MgCO}_3} + n^{\text{D}}_{\text{MgCO}_3} - n^{\text{HM}}_{\text{C}}. \qquad [2]$$

Post-combustion occurs at the top of the melter gasifier. In this work, we use the degree of

post-combustion reactions, as defined by Fruehan *et al.*[39]:

$$\text{pcr} = \frac{[\text{pct}CO_2 + \text{pct}H_2O]}{[\text{pct}CO + \text{pct}CO_2 + \text{pct}H_2 + \text{pct}H_2O]} \times 100. \quad [3]$$

The composition of the gas leaving the melter gasifier is calculated using Eq. [3], which gives the composition of the surplus gas. In the reduction shaft, the ore is reduced to Fe and $Fe_{0.95}O$ in the Fe:$Fe_{0.95}O$ molar ratio. This is known as the degree of metallization, and it is labeled X in this work.

The reduction of iron oxides in H_2/H_2O and CO/CO_2 atmosphere follows the reactions given below. Here the (CO/CO_2) reactions are given in parentheses. $+\Delta H$, signifies the endothermic, and $-\Delta H$, signifies the exothermic reaction:

$$3Fe_2O_3 + H_2(CO) = 2Fe_3O_4 + H_2O(CO_2) \quad \text{with,} \quad -\Delta H(+\Delta H)$$
$$Fe_3O_4 + H_2(CO) = 3FeO + H_2O(CO_2) \quad \text{with,} \quad +\Delta H(+\Delta H)$$
$$FeO + H_2(CO) = Fe + H_2O(CO_2) \quad \text{with,} \quad +\Delta H(-\Delta H)$$

The Bauer–Glaessner diagram, which represents the chemical reactions, as presented above, are plotted for different temperatures and partial pressures of hydrogen and carbon monoxide in Figure 2.[40] As is obvious from the diagram, below 810 °C, the reduction ability of hydrogen is lower than that of carbon monoxide. Nevertheless, above 810 °C, the reduction ability of hydrogen is higher. Therefore, reduction by hydrogen above 810 °C, and by carbon monoxide below it, is more evidently efficient. At 1000 °C, Fe-O-C and Fe-O-H equilibrium curves show that the equilibrium concentration of CO formed when Fe_3O_4 reduces to wustite is 20 pct and for wustite to Fe reduction is about 70 pct. Therefore, the amount of utilization of CO and H_2 is at a maximum of 80 and 63 pct for magnetite/wustite equilibrium. Yet for the wustite to iron equilibrium, the utilization efficiency is only 30 and 37 pct, respectively. The reaction for wustite reduction by CO, and similarly for reduction by H_2, may be written as follows:

$$Fe_{0.95}O + 3.3CO = 0.95Fe + CO_2 + 2.3CO$$
$$Fe_{0.95}O + 2.7H_2 = 0.95Fe + H_2O + 1.7H_2$$

Therefore the ($CO + H_2$) requirement for the melter gasifier to operate at X pct metallization is given by:

$$n_{CO}^{req} = \left(\frac{X}{100}\right)\left(\frac{3.3 - 1.22n_{H_2}^{r}}{0.95}\right) \quad [4]$$

$$n_{H_2}^{req} = \left(\frac{X}{100}\right)\left(\frac{n_{H_2}^{r}}{0.95}\right) \quad [5]$$

When the required CO and H_2 is added to the gas coming from the melter gasifier (determined using Eqs. [4] and [5]), the gas is sent to the reduction shaft for pre-reduction of the ore to the required degree of metallization. Utilization of CO and H_2 at 1200 K (923 °C) for $Fe_{0.95}O$ to Fe reduction is 30 and 37 pct, respectively. This in fact will directly yield the top gas composition.

The oxygen required for post-combustion is calculated using pcr. The amount of oxygen required for coal combustion is calculated using oxygen balance, as given in Eq. [6]:

$$n_O^{bal} = n_O^{sg} + n_O^{tg} - n_O^{pc} - n_O^{ore} - 2 \times \left[n_{CaCO_3}^{L} + n_{CaCO_3}^{L} + n_{MgCO_3}^{D} + n_{MgCO_3}^{D}\right] - n_O^{coal} - n_O^{M}. \quad (6)$$

B. *Heat Balance*

Heat is produced in both the coal combustion and the post-combustion stage. This heat is consumed by the energy demands in the melter gasifier and the reduction shaft. Heat accumulation should be zero for a steady-state process. Heat demand in the melter gasifier can be determined by summing up the heats required for (1) raising the temperature of hot metal and slag to a taping temperature, (2) formation of slag, (3) mixing of hot metal, (4) endothermic reactions, (5) drying of coal, (6) devolatilization of coal, along with (7) heat carried away by gas leaving the melter gasifier and (8) miscellaneous dissipation losses. This is captured using Eqs. [7] through [11]. Sensible heat and heat of mixing of hot

Table I. Elements Entering and Leaving the Process

Elements	Entering the Process	Leaving the Process
C	coal, coke, limestone, dolomite	hot metal, top gas, surplus gas
Fe	ore	hot metal
Si	ore, coal ash, coke ash, limestone, dolomite	hot metal, slag
Mn	ore	hot metal
S	ore	hot metal, slag
P	ore	hot metal
H	coal	top gas, surplus gas
Ca	coal, ash, coke ash, limestone, dolomite	slag
O	ore, limestone, dolomite, coal moisture, tuyere and secondary air	top gas, surplus gas, slag
N	coal, secondary air	top gas, surplus gas
Mg	limestone, dolomite	slag
Al_2O_3	ore, coal ash, coke ash, limestone, dolomite	slag

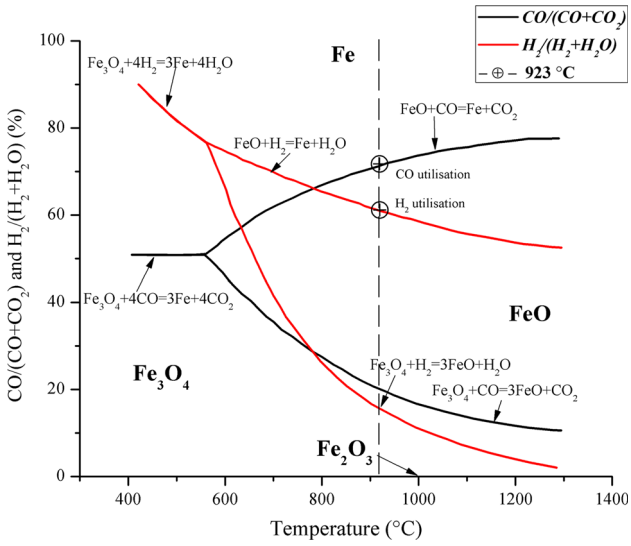

Fig. 2—Combination of Baur–Glaessner diagrams for H_2/H_2O and CO/CO_2 atmosphere (Adapted from Gudenau *et al.*[40]).

metal constituents gives the "hot metal heat demand" given below:

$$\Delta H_{\mathrm{HM}} = \Delta H_{\mathrm{s}}^{\mathrm{HM}} + \Delta H_{\mathrm{m}}^{\mathrm{HM}} \quad [7]$$

The slag's heat demand is given by the sum of (1) sensible heat of slag and (2) heat of slag formation. The heat of slag formation includes the formation of complexes, namely, $2CaO{\cdot}Al_2O_3{\cdot}SiO_2$, $2CaO{\cdot}Al_2O_3$, $CaO{\cdot}SiO_2$, $MnO{\cdot}SiO_2$, and $2MgO{\cdot}SiO_2$, per kg-mole of Fe:

$$\Delta H_{\mathrm{slag}} = \Delta H_{\mathrm{s}}^{\mathrm{slag}} + \Delta H_{\mathrm{f}}^{\mathrm{slag}} \quad [8]$$

It may be noted that the comprehensive list of endothermic reactions occurring in the melter gasifier includes (1) reduction of $Fe_{0.95}O$, MnO, SiO_2, and P_2O_5, using C, and (2) decomposition of $CaCO_3$ and $MgCO_3$ to release CO_2. The total heat absorbed by all the endothermic reactions put together is estimated by simply summing up all the individual heat requirements:

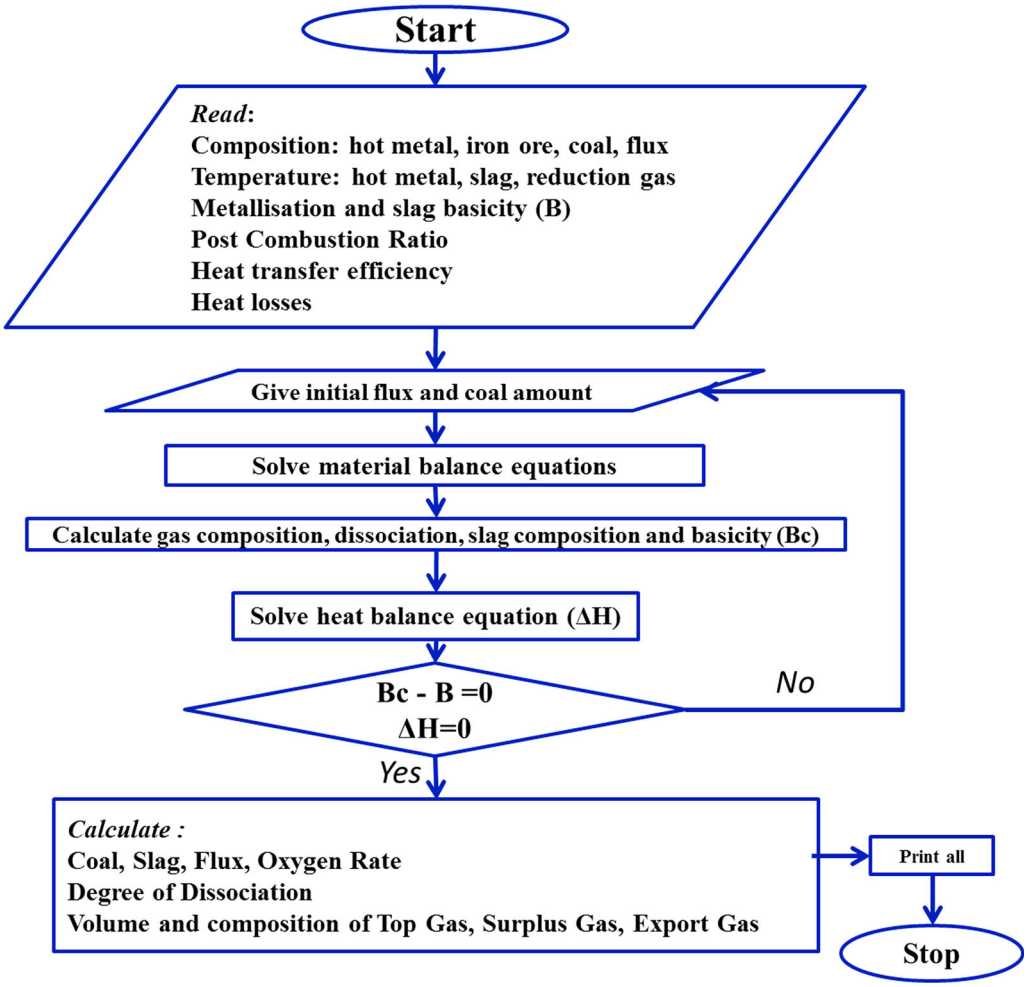

Fig. 3—Flow chart of the model.

Table II. Input Parameters of the Model as Prescribed by JSW Plant Data

Ore Composition (in Pct)	Fe_2O_3	90.357
	Mn	01.006
	P_2O_5	01.598
	FeS	00.006
	SiO_2	04.420
	Al_2O_3	02.560
Coke Composition (in Pct)	C	86.39
	S	00.70
	Ash	12.64
Ash Composition (in Pct)	SiO_2	41.22
	Al_2O_3	25.62
	CaO	10.19
	MgO	02.17
Blend of Coal (in Pct)	Avani coal	35
	Ensham coal	30
	Namoi coal	35
Avani Coal Composition (in Pct)	C	61.37
	H	04.0512
	O	12.32
	N	00.422
	S	00.36
	P	00.0844
	moisture	12.20
	ash	09.19
Ensham Coal composition (in Pct)	C	58.53
	H	04.2096
	O	12.8042
	N	00.4385
	S	00.64
	P	00.0877
	moisture	10.60
	ash	12.69
Namoi Coal Composition (in Pct)	C	61.46
	H	04.3824
	O	13.3298
	N	00.4565
	S	00.41
	P	00.0913
	moisture	11.60
	ash	08.27
Limestone Composition (in Pct)	$CaCO_3$	95.63
	$MgCO_3$	20.00
	SiO_2	01.03
	Al_2O_3	00.34
Dolomite Composition (in Pct)	$CaCO_3$	45.2767
	$MgCO_3$	38.573
	SiO_2	11.79
	Al_2O_3	02.75
Hot Metal Composition (in Pct)	C	04.19
	Si	01.37
	Mn	00.083
	S	00.049
	P	00.116
Temperature (in K)	hot metal	1756
	reducing gas	1073
	top gas	593
	pre-reduced ore	1200
Slag Basicity	Bc	1.2

$$\Delta H_e = \Delta H_e^{Fe_{0.95}O} + \Delta H_e^{MnO} + \Delta H_e^{SiO_2} + \Delta H_e^{P_2O_5} + \Delta H_e^{CaCO_3} + \Delta H_e^{MgCO_3} \quad [9]$$

Heat carried away by the gas leaving the melter gasifier is calculated by (1) taking into account its sensible heat and (2) adding the heat of the surplus gas that enters:

$$\Delta H_s^{gas} = \Delta H_s^{CO} + \Delta H_s^{CO_2} + \Delta H_s^{H_2} + \Delta H_s^{H_2O} + \Delta H_s^{N_2} \quad [10]$$

The model considers a heat loss Q_{MG} of 5 to 8 pct of the total heat demand. This too is added to the actual heat demand to calculate total heat demand (the actual percentage of heat loss is calculated after suitable validation using industrial data):

$$\Delta H_{dem} = \Delta H_{HM} + \Delta H_{slag} + \Delta H_e + \Delta H_s^{gas} + \Delta H_{coal} + \Delta H_{DVC} + Q_{MG} \quad [11]$$

Akin to the equations given above, the total heat supplied to the melter gasifier by coal combustion and post-combustion may be written as follows:

$$\Delta H_{sp} = \Delta H_{sp}^{coal} + \Delta H_{sp}^{pc}. \quad [12]$$

III. METHOD OF CALCULATION

A computer program is developed using the thermochemical model described above. This system of equations enables accurate reasonable calculation of coal rate, flux rate, slag rate, oxygen requirement, and export gas as a function of the degree of metallization and post-combustion ratio. Figure 3 shows the flow chart of the computer program. With the provision of initial guess values of mass of coal and flux, it calculates the kg moles of material entering and leaving the process (per kg-mole of Fe product). Material balance equations are solved to obtain gas and slag composition, and slag basicity (*Bc*). *Bc* is readily determined using the following (Eq. [13]):

$$Bc = \frac{n_{CaO}^{slag} + n_{MgO}^{slag}}{n_{SiO_2}^{slag} + n_{Al_2O_3}^{slag}} \quad [13]$$

The values of mass of coal and flux are iterated through the self-consistent loop that is set up. The heat and material balances are performed until calculated basicity (*Bc*) and heat demand (ΔH_{dem}) matches with a given basicity (*B*) and heat supplied (ΔH_{sp}), respectively.

Table III. Heat Balance of the Reduction Shaft Furnace

Heat Input (GJ/Ton)		Heat Output (GJ/Ton)	
Sensible heat of reducing gas entering shaft furnace	2.23	sensible heat of top gas leaving shaft furnace	0.73
		sensible heat of material delivered to melter gasifier	0.83
		endothermic heat of reaction inside shaft furnace	0.23
		heat losses in shaft furnace	0.44
Total	2.23	total	2.23

Table IV. Heat Balance of the Melter Gasifier

Heat Input (GJ/Ton)		Heat Output (GJ/Ton)	
Sensible heat of material delivered from shaft furnace	0.83	sensible heat of hot metal	1.39
Heat of formation of slag	0.07	sensible heat of slag	0.54
Heat of reaction of coal combustion	7.10	sensible heat of reducing gas leaving melter gasifier	2.35
Heat of reaction of post-combustion	2.08	endothermic heat of reactions in melter-gasifier	3.22
		coal drying heat	1.50
		latent heat of devolatization of coal	0.60
		heat losses in melter gasifier	0.48
Total	10.08	total	10.08

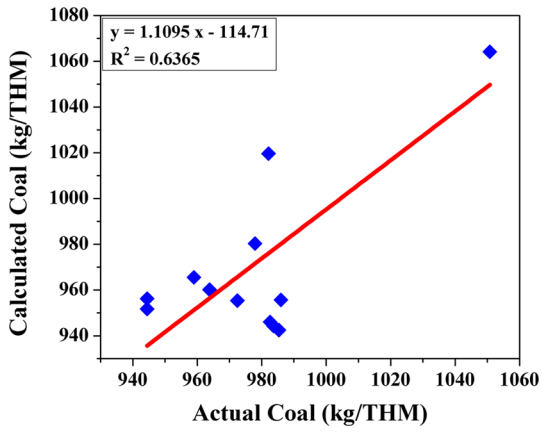

Fig. 4—Actual *vs* calculated coal consumption (kg/THM).

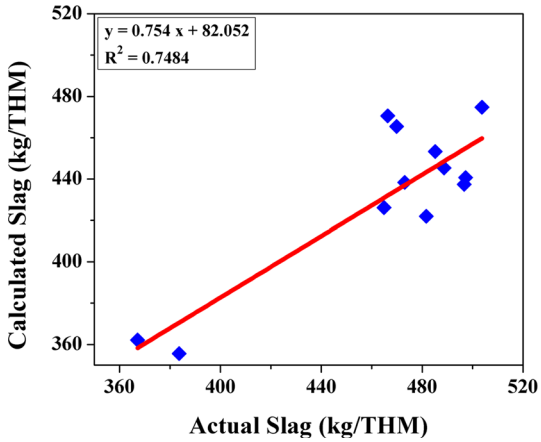

Fig. 6—Actual *vs* calculated slag produced (kg/THM).

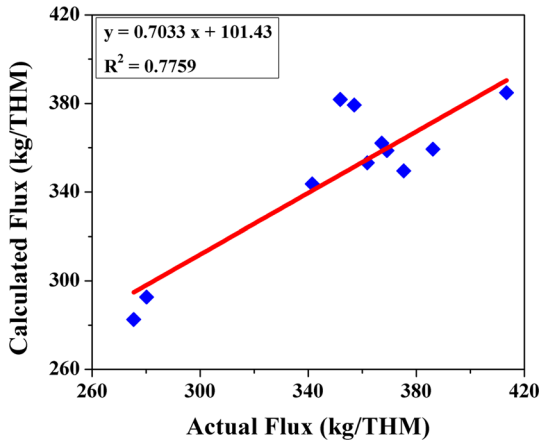

Fig. 5—Actual *vs* calculated flux consumption (kg/THM).

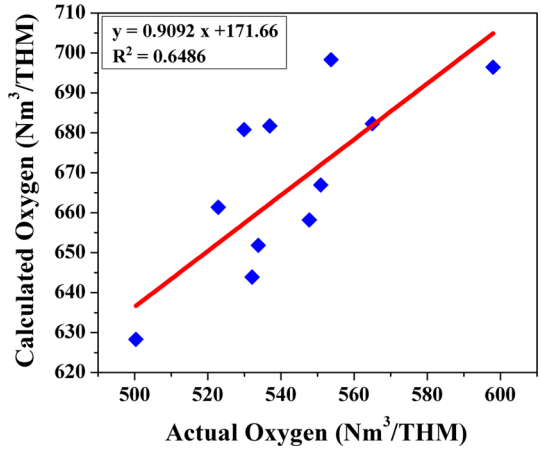

Fig. 7—Actual *vs* calculated oxygen consumption (Nm^3/THM).

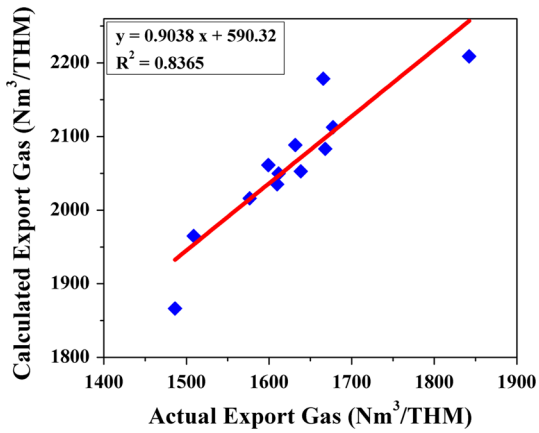

Fig. 8—Actual *vs* calculated export gas generated (Nm^3/THM).

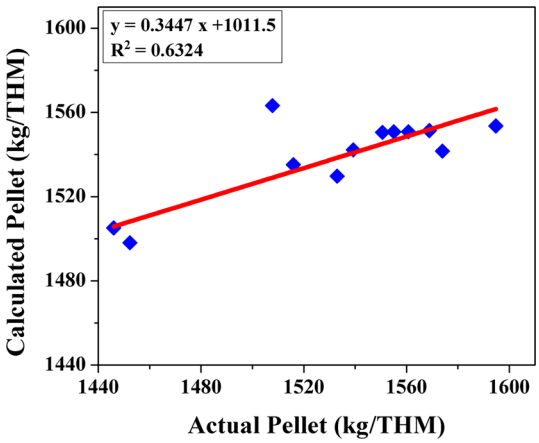

Fig. 9—Actual *vs* calculated pellets consumed (kg/THM).

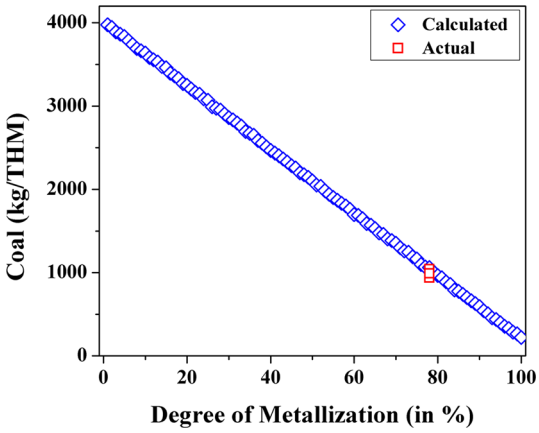

Fig. 10—Coal required with respect to increase in degree of metallization.

IV. RESULTS AND DISCUSSION

Material balance and heat balance is carried out by specifying X, pcr, and assuming the initial mass of coal (M_C) and flux ($M_L + M_D$). The coal amount and flux amount thus obtained are used to calculate the gas composition, slag composition, and slag basicity (Bc). The coal rate (kg/THM), flux rate (kg/THM), and slag rate (kg/THM) are also calculated for different operating conditions using the model presented in this work.

($CO + H_2$) required in the reduction shaft for reduction of hematite to wustite is the amount of ($CO + H_2$) left in the surplus gas. The oxygen requirement for post-combustion and coal combustion is calculated by adding the kg moles of CO_2 and H_2O in the melter gasifier and the oxygen balance in the melter gasifier, respectively. Similarly, top gas, surplus gas, and total export gas amount and compositions (CO, CO_2, H_2, H_2O, and N_2) are also calculated. The input and output heat values for the reduction shaft and melter gasifier, calculated using the data obtained from Table II, has been tabulated in Tables III and IV, respectively.

A. *Validation of the Model*

The model has been validated using the data obtained from the COREX plant, JSW Toranagallu, India. The program has been tested for the data collected over a period of 20 days. The correlation between actual plant data and model values are presented. Figures 4 through 9 show the amount of coal required, flux required, slag produced, oxygen required, export gas generated, and pellets consumed, calculated using the model. Benchmarking is done using the plant data of the corresponding day. The results calculated by the model are in reasonable agreement with the industrial data for the metallization value of 78 pct and a post-combustion of ratio of 20 pct.

B. *Variation of Degree of Metallization*

The model predicts the variation of input raw material needed and the corresponding by-product produced with respect to changes in the degree of metallization and post-combustion ratio. Plant data for an arbitrary day, as shown in Table I, have been used. By varying the degree of metallization from 0 to 100 pct, and by keeping the post-combustion ratio constant at 20 pct, the variations in the process parameters are plotted. Figure 10 shows the amount of coal required for different degrees of metallization. When no metallization occurred in the reduction shaft, the process requires 4000 kg/THM of coal, thus, leading a coal-based single stage smelting reduction process. At 100 pct metallization, a minimal amount of coal (~ 100 kg/THM) is required, which will be used for smelting of DRI coming from the reduction shaft.

The behavior observed in Figure 11 shows that the degree of metallization influences the required flux amount. We note that the flux amount is 570 kg/THM at no metallization, and it becomes 150 kg/THM at 100 pct metallization. The decrease in the required amount of flux with an increase in degree of metallization can be attributed to the fact that more coal brings more ash into the system. The decrease in flux amount results in a decrease in the amount of slag generated. Justification of this behavior is observed in Figure 12, which shows 200 kg/THM of slag for 100 pct

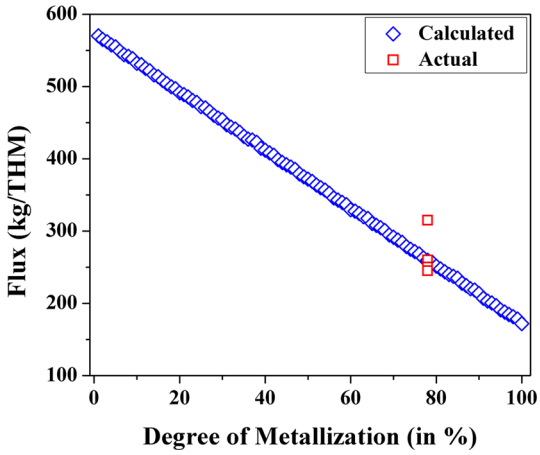

Fig. 11—Flux required with respect to increase in degree of metallization.

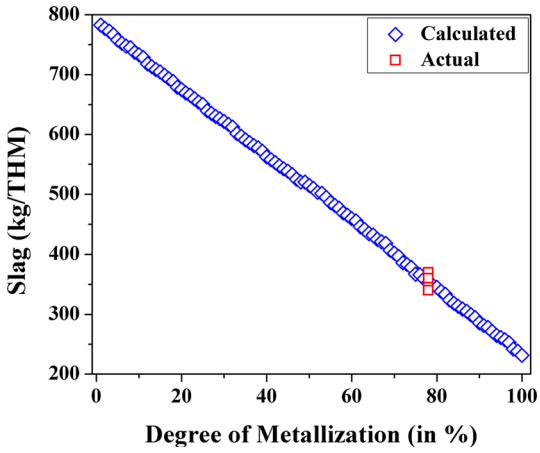

Fig. 12—Slag produced with respect to increase in degree of metallization.

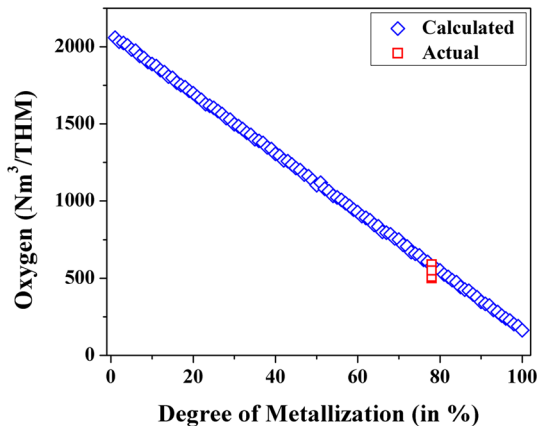

Fig. 13—Oxygen required for coal combustion with respect to increase in degree of metallization.

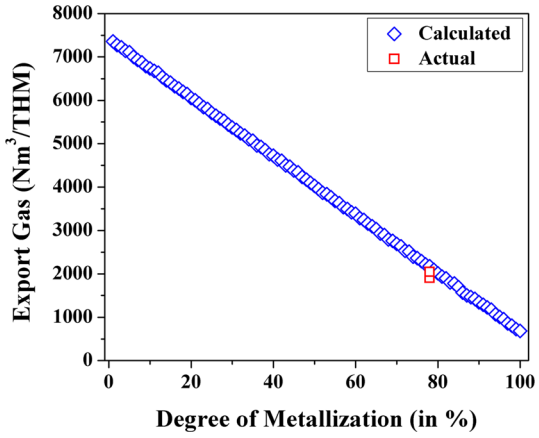

Fig. 14—Net export gas generated with respect to increase in degree of metallization.

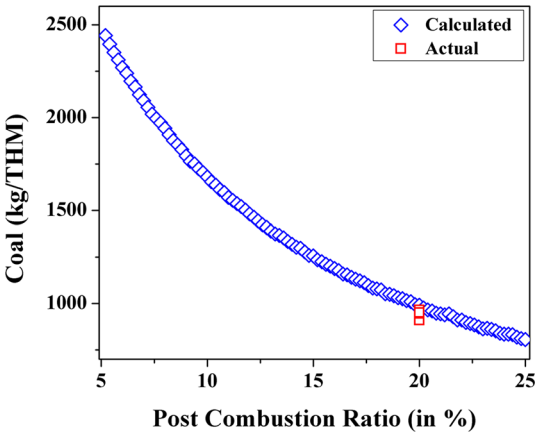

Fig. 15—Coal required with respect to increase in post-combustion ratio.

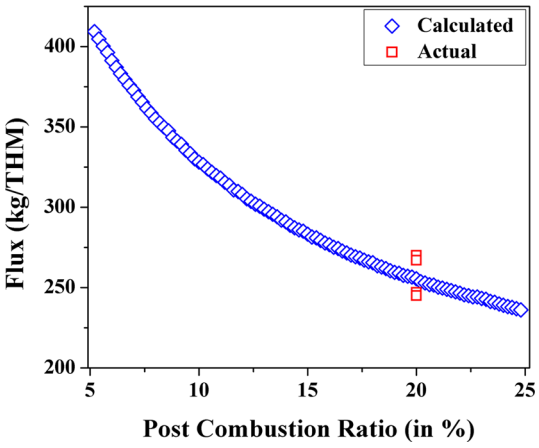

Fig. 16—Flux required with respect to increase in post-combustion ratio.

metallization and 800 kg/THM for no metallization. The amount of oxygen required for coal combustion is also directly proportional to the amount of coal that is fed into the system. Figure 13 shows that 2000 Nm^3/THM of oxygen is required for no metallization, which decreases to 100 Nm^3/THM for 100 pct metallization. Figure 14 shows the variation of total export gas generated from the COREX plant with respect to the

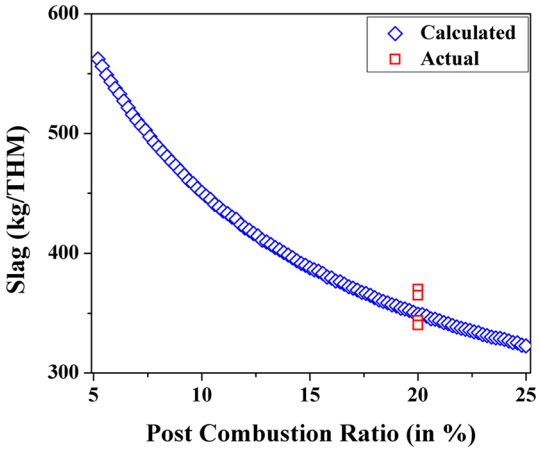

Fig. 17—Slag produced with respect to increase in post-combustion ratio.

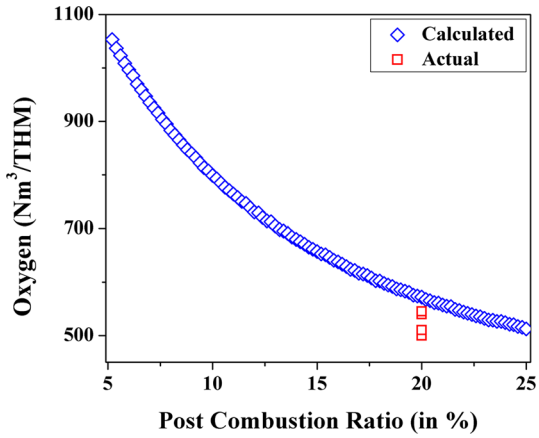

Fig. 18—Oxygen required for coal combustion with respect to increase in post-combustion ratio.

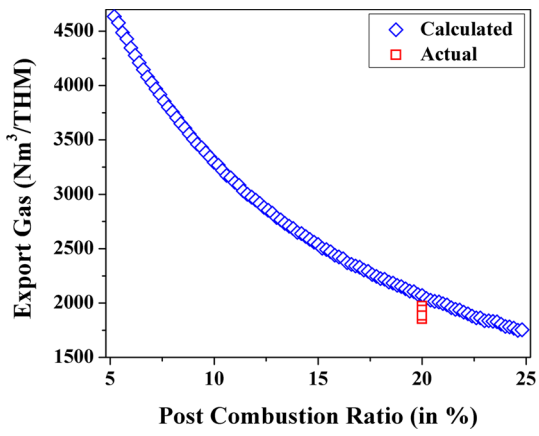

Fig. 19—Net export gas generated with respect to increase in post-combustion ratio.

degree of metallization: 7100 Nm^3/THM of net export gas is generated for 0 pct metallization, and 700 Nm^3/THM is produced at 100 pct metallization. This is due to the net effect of a decrease in the amount of reducing gas needed as metallization increases.

C. *Variation of Post-combustion Ratio*

The variations in the process parameters are plotted for variations in the post-combustion ratio from 5 to 25 pct, while the degree of metallization is kept constant at 78 pct. As the degree of metallization is kept constant, extra gas will be required in the reduction shaft for increasing the post-combustion ratio. The coal is required only to satisfy heat demand by coal combustion and post-combustion.

As post-combustion ratio increases from 5 to 25 pct, the amount of coal required decreases from 2400 to 800 kg/THM, as shown in Figure 15. Coal is the prime source of ash entering into the system. Thus, an increase in post-combustion ratio will result in a decrease in the amount of ash entering the system. The amount of slag generated, and the flux required, will also decrease with a decrease in the ash content. This behavior is evident from Figures 16 and 17. Figure 16 shows the flux rate decreases from 410 to 240 kg/THM. Figure 17 shows that the amount of slag generated also decreases from 560 to 325 kg/THM for an increase in post-combustion ratio from 5 to 25 pct. An increase in the gas being post-combusted leads to a decrease in the amount of coal required, thus, lowering the need oxygen for coal combustion. Figure 18 shows a result that is consistent with this and shows a decrease in the oxygen required for coal combustion from 1050 to 500 Nm^3/THM. Total export gas decreases from 2600 to 1800 Nm^3/THM for an increase in a post-combustion ratio from 5 to 25 pct. From Figure 19, it can be seen that there is a trend in showing a decrease in the amount of reducing gas coming from the melter gasifier with an increase in post-combustion ratio.

V. CONCLUSION

A thermochemical model has been developed to describe the Corex process. The model predicts the requirement of raw materials as well as the volumes of generated waste slag and top gases. Based on benchmarking using industrial data provided by JSW Steel Ltd., we show that the calculated results are in good agreement for a metallization of 78 pct and post-combustion of 20 pct (R^2 ~ 0.65 to 0.80). It means that ~ 80 pct of the predicted results are in close agreement with actual observations; hence, the trends shown in this work are very likely relevant for engineers working with optimization of the Corex process. Nevertheless, some caution may be exercised while directly deducing precise changes to process variables using our results since process plant data often suffer from variations and uncertainties due to variance in raw material composition and measurement errors. Yet, by and large, the predictive model presented here can be clearly used as a guiding tool to predict the raw material requirement for the COREX process.

The effects of metallization and post-combustion have been studied with the help of the model presented here. In general, an increase in the degree of metallization decreases coal, flux, and oxygen requirements, and it

reduces the export gas produced substantially. An increase in the post-combustion ratio (from 5 to 25 pct) reduces coal combustion by 80 pct, thus, reducing the coal, flux, and oxygen requirement by 50 pct. It is therefore recommended that the degree of metallization be above ~ 70 pct and the post-combustion ratio be ~ 20 pct. At a higher post-combustion ratio, CO_2 dissociation occurs, thus, increasing the temperature and increasing the H_2 consumption for post-combustion. Coal consumption is also low (~ 900 kg/THM) for a high post-combustion ratio (~ 20 pct).

It has been concluded that the COREX process is evidently more economical and environmentally friendly for high metallization (~ 70 pct or more) and post-combustion ratios (~ 20 pct). The predicted data are expected to enable comprehensive analysis of process variables chosen, and they can predict an impact on output parameters (with ~ 80 pct accuracy). Nevertheless, we notice fundamental thermodynamic limitations in our analysis: (1) shaft furnace as far as attainment of high metallization is concerned and (2) in the melter gasifier as far as attainment of high post-combustion is concerned. Such limitations can be addressed by developing a suitable kinetic model, which will be the next step in the current work.

ACKNOWLEDGMENTS

The authors would like to acknowledge JSW Steel Ltd., Toranagallu, Bellary, India, for providing the plant data.

NOMENCLATURE

ABBREVIATIONS

THM	1 ton of hot metal

SYMBOLS

n_a^b	Amount (in kg-mole) of any "a" in "b", per kg-mole of Fe
p_a^b	Composition of any "a" in "b" (in wt pct)
M_a	Moisture content in "a"
X	Degree of metallization (in mol pct)
pcr	Post-combustion ration (in vol pct)
ΔG	Gibbs-free energy (kJ)
Bc	Slag basicity
B	Actual basicity
T	Temperature (K)
ΔH_m	Heat of mixing per kg-mole of Fe (kJ)
ΔH_s	Sensible heat per kg-mole of Fe (kJ)
ΔH_f	Heat of formation per kg-mole of Fe (kJ)
ΔH_e	Heat of endothermic reaction per kg-mole of Fe (kJ)

SUPERSCRIPTS AND SUBSCRIPTS

coal	Coal
L	Limestone
D	Dolomite
HM	Hot metal
slag	Slag
ore	Ore
sg	Surplus gas
tg	Top gas
pc	Post-combustion
mg	Gas from the melter gasifier
r	Reducing gas
MG	Melter gasifier
DVC	Devolatization of coal
sp	Supplied
dem	Demanded
o	Output
A	Active

REFERENCES

1. A. Hasanbeigi, M. Arens, and L. Price: *Renew Sustain. Energy Rev.*, 2014, vol. 33, pp. 645–58.
2. T. Kuramochi, A. Ramírez, W. Turkenburg, and A. Faaij: *Prog. Energy Combust. Sci.*, 2012, vol. 38, pp. 87–112.
3. X.L. Zhou and Z.N. Du: *Adv. Mater. Res.*, 2013, vols. 774–6, pp. 1430–33.
4. J.K. Wright, I.F. Taylor, and D.K. Philp: *Miner. Eng.*, 1991, vol. 4, pp. 983–1001.
5. M.K. Shin, J.K. Yoon, and M. Tokuda: *ISIJ Int.*, 1993, vol. 33, pp. 385–90.
6. S.C. Lee, M.K. Shin, S. Joo, and J.K. Yoon: *ISIJ Int.*, 1999, vol. 39, pp. 319–28.
7. S.C. Lee, M.K. Shin, S. Joo, and J.K. Yoon: *ISIJ Int.*, 2000, vol. 40, pp. 1073–79.
8. S. Pal and A.K. Lahiri: *Metall. Mater. Trans. B*, 2003, vol. 34B, pp. 103–14.
9. S. Pal and A.K. Lahiri: *ISIJ Int.*, 2006, vol. 46, p. 58.
10. S. Pal and A.K. Lahiri: *Metall. Mater. Trans. B*, 2003, vol. 34B, pp. 115–19.
11. S. Wu, J. Xu, S. Yang, Q. Zhou, and L. Zhang: *ISIJ Int.*, 2010, vol. 50, pp. 1032–39.
12. S. Wu, J. Xu, J.I. Yagi, X. Guo, and L. Zhang: *ISIJ Int.*, 2011, vol. 51, pp. 1344–52.
13. J. Xu, S. Wu, M. Kou, and K. Du: *ISIJ Int.*, 2013, vol. 53, pp. 576–82.
14. M. Kou, S. Wu, K. Du, W. Shen, J. Sun, and Z. Zhang: *ISIJ Int.*, 2013, vol. 53, pp. 1002–09.
15. M. Kou, S. Wu, W. Shen, K. Du, L. Zhang, and J. Sun: *ISIJ Int.*, 2013, vol. 53, pp. 2080–89.
16. M. Kou, S. Wu, K. Du, W. Shen, X. Ma, M. Chen, and B. Zhao: *JOM*, 2015, vol. 67, pp. 459–66.
17. M. Kou, S. Wu, G. Wang, B. Zhao, and Q. Cai: *Steel Res. Int.*, 2015, vol. 86, pp. 686–94.
18. H. Zhou, Z.G. Luo, T. Zhang, Y. You, Z.S. Zou, and Y. Shen: *ISIJ Int.*, 2016, vol. 56, pp. 245–54.
19. M.H. Bai, S.F. Han, W.Y. Zhang, K. Xu, and H. Long: *Ironmak. Steelmak.* 2016, pp. 1–7.
20. Q. Hou, J. Li, and A. Yu: *Steel Res. Int.*, 2015, vol. 86, pp. 626–35.
21. W. Ying, Y. Sun, Z. Luo, and Z. Zou: *Adv. Mater. Res.*, 2011, vols. 287–90, pp. 827–30.

22. S. Sarkar and G.S. Gupta: *Metall. Mater. Trans. B*, 2007, vol. 38B, pp. 965–75.
23. G. Pan, X.L. Liu, and Z. Wen: *Ironmak. Steelmak.*, 2013, vol. 40, pp. 255–62.
24. J. Sun, Z. Luo, and Z. Zou: *Powder Technol.*, 2015, vol. 281, pp. 159–66.
25. S.C. Barman, K.P. Mrunmaya, and M. Ranjan: *J. Iron Steel Res. Int.*, 2011, vol. 18, pp. 20–24.
26. H.F. Li, Z.G. Luo, Z.S. Zou, J.J. Sun, L.H. Han, and Z.X. Di: *J. Iron Steel Res. Int.*, 2012, vol. 19, pp. 36–42.
27. B. Srivastava, S.K. Roy, and P.K. Sen: *Metall. Mater. Trans. B*, 2010, vol. 41B, pp. 935–39.
28. O. Almpanis-Lekkas, B. Weiss, and W. Wukovits: *J. Clean. Prod.*, 2015, pp. 1–11.
29. P. Sen, C. Biswas, P. Das, and G.G. Roy: *Trans. Inst. Min. Metall. Sect. C*, 2015, vol. 124, pp. 175–83.
30. A. Kadrolkar, S.K. Roy, and P.K. Sen: *Metall. Mater. Trans. B*, 2012, vol. 43B, pp. 173–85.
31. X. Liu, G. Pan, G. Wang, and Z. Wen: *Energy Fuels*, 2011, vol. 25, pp. 5729–35.
32. G. Pan, X.L. Liu, and Z. Wen: *Adv. Mater. Res.*, 2011, vols. 228–9, pp. 930–36.
33. G. Pan, Z. Wen, X.L. Liu, Y.K. Li, K.C. Zheng, and W.F. Wu: *Ironmak. Steelmak.*, 2015, vol. 42, pp. 489–97.
34. K. Du, S. Wu, M. Kou, W. Shen, and Z. Zhang: *Steel Res. Int.*, 2014, vol. 85, pp. 466–76.
35. L.H. Han, Z.-G. Luo, H. Zhou, Z.-S. Zou, and Y.-Z. Zhang: *J. Iron Steel Res. Int.*, 2015, vol. 22, pp. 304–10.
36. S.C. Koria, M.K. Barui, and L.K. Pandey: *Scand. J. Metall.*, 1999, vol. 28, pp. 17–24.
37. S.C. Koria and M.K. Barui: *Ironmak. Steelmak.*, 2000, vol. 27, pp. 348–54.
38. Y. Qu, Z. Zou, and Y. Xiao: *ISIJ Int.*, 2012, vol. 52, pp. 2186–93.
39. R.J. Fruehan, K. Ito, and B. Ozturk: *Steel Res.*, 1989, vol. 60, pp. 129–37.
40. H.W. Gudenau, D. Senk, S. Wang, K. De Melo Martins, and C. Stephany: *ISIJ Int.*, 2005, vol. 45, pp. 603–08.